An Experimental Investigation and Linear, Nonlinear Finite Element Analysis of the 1/10th Scale Model of Prestressed Concrete Reactor Vessel

Wang Tai-Jun

Institute of Nuclear Energy Technology

Wang Chuan-Zhi

Dept. of Civil and Environmental Engineering

Xia Zhi-Xi

Dept. of Applied Mechanics

Gu Shu-Xi, He Shu-Yan, Xiong Dun-Shi, Li Jing-Cai, Lio Jun-Jie

Institute of Nuclear Energy Technology
Tsinghua University, P.O. Box 1021, Beijing, P.R. of China

Abstract

In this paper, the result of the tests of 1/10th scale model of PCRV in elastic range, cracked condition and ultimate loading condition are shown. The linear, nonlinear stress analysis and ultimate load of the model are also presented. In the linear analysis, 3D finite elements with arbitrarity arranging nodes were used, and in the nonlinear analysis axi-symmetric (3D) finite elements were used. The interaction of linear, prestressing cable, rebar and concrete solid are considered in both analysis. The ultimate load of PCRV was calculated by using the yield line method.

There were generally good agreements between the test results and theoretical predictions.

1. Introduction

The 1/10th PCRV model was a cylindrical vessel with thick end slab in flat form and the prestress was provided by a helical tendon system as it was used in the PCRV of Hinkley Point B Power Station Fig. 1. The prestresses system consists of 180 No. 7Ø4 stands, and every three 7Ø4 stands were formed a tendon, so that the average anchorage load of each tendon was 23 tonnes which is 70% GUTS. A special lubricant was used to decreased the loss of prestressed. All of these tendons were arranged into four layers in the barrel. A sealed steel liner with 0.04m in thick, 0.9m in diameter and 0.9m in height was put in the cylinder to exert interior pressure loading and was used to maintain the seal integrality. The nomal working interior pressure was 40kg/cm^2 and the design interior pressure was assumed as 44kg/cm^2. The designed ultimated pressure is 110kg/cm^2 which is 2.5 times the design pressure.

The specified concrete compressive strength(cubic specimen) was 400 kg/cm^2 to 500 kg/cm^2 and Young's modulus was 300,000 and 330,000 kg/cm^2. The coarse aggregate was 5-12mm natural gravel.

The pressure tests were conducted with pumped water. After several elastic range tests up to the design pressure, the cracking range test and the ultimate pressure test, including proof pressure stage (1.15 times design pressure), were carried out.

Mechanical dials and electronic transducers were used to measure deformations. Strains gages were placed on the surface and embedded into the concrete to measure strains of concrete. Loading transducers are placed under the anchorages to measure the forces in the prestressing cables. The whole experimental process was recorded using four cameras which were arranged in different positions.

The measured behaviour of the model was compared with the 3D linear and axi-symmetric(3D) nonlinear finite element analysis to ensure the validity of the analytical methods.

2. Stress analysis

2.1 Elastic stress analysis by three-dimensional isoparametric finite element method

Taking into consideration of the effect of the liner, the membrane and bar element were used, and rebar and prestressed reinforcement, the elastic solution of a PCRV by 3D isoparametric finite element method was presented. The isoparametric hexahedron and pentahedron elements with different nodes were used. The nodes of hexahedron may be from 8 to 36, and the nodes of pentahedron may be from 6 to 27. The nodes of each boundary of elements may be from 2 to 5.[3]

2.1.1 The calculation of shape functions of different elements[4]

The hexahedron, pentahedron and quadrihedron elements with corresponding corner nodes may be considered as their basic elements respectively. Adding m nodes to the sides of these basic elements, a set of new higher order elements, which have higher degree of freedom, will be obtained. The new shape functions will be calculated as following,

$$N_i = N_i^{\circ} - \sum_{j=n+1}^{n+m} N_{ij}^{\circ} N_j \qquad (1)$$

where, N_i -- the shape function of corner node i; N_i° -- the shape function of corner node of basic elements; N_{ij} -- the value of shape function at node j of N_i° ; N_j -- the shape function of boundary node j, which well obtained by using the modified Lagrange interpolation method. n-- the total numbers of corner nodes; m-- the total number of side nodes.

2.1.2. The calculation of stiffness matrix of membrane elements

According to usual process, the stiffness of membrane element may be calculated as following,

$$K_m = t\iint [B]^T [L_m]^T [D_m][L_m][B]\sqrt{r_x^2 + r_y^2 + r_z^2}\, d\xi\, d\eta \qquad (2)$$

where, ξ, η = the local coordinate of membrance elements.
$[B]$ = the geometic matrix of solid elements

$[L_m]$ = the matrix of coordinate tranlation

$$[L_m] = \begin{bmatrix} l_1^2 & m_1^2 & n_1^2 & l_1 m_1 & m_1 n_1 & n_1 l_1 \\ l_2^2 & m_2^2 & n_2^2 & l_2 m_2 & m_2 n_2 & n_2 l_2 \\ 2l_1 l_2 & 2m_1 m_2 & 2n_1 n_2 & l_1 m_1 + l_2 m_2 & m_1 n_1 + m_2 n_2 & n_1 l_1 + n_2 l_2 \end{bmatrix}$$

$$l_1 = \frac{1}{a_1}\frac{\partial X}{\partial \xi}, \qquad m_1 = \frac{1}{a_1}\frac{\partial Y}{\partial \xi}, \qquad n_1 = \frac{1}{a_1}\frac{\partial Z}{\partial \xi},$$

$$l_2 = \frac{1}{a_2}\frac{\partial X}{\partial \eta}, \qquad m_2 = \frac{1}{a_2}\frac{\partial Y}{\partial \eta}, \qquad n_2 = \frac{1}{a_2}\frac{\partial Z}{\partial \eta}.$$

$$a_1 = \sqrt{\left(\frac{\partial X}{\partial \xi}\right)^2 + \left(\frac{\partial Y}{\partial \xi}\right)^2 + \left(\frac{\partial Z}{\partial \xi}\right)^2} \qquad a_2 = \sqrt{\left(\frac{\partial X}{\partial \eta}\right)^2 + \left(\frac{\partial Y}{\partial \eta}\right)^2 + \left(\frac{\partial Z}{\partial \eta}\right)^2}$$

$$M_x = \frac{\partial Y}{\partial \xi}\cdot\frac{\partial Z}{\partial \eta} - \frac{\partial Z}{\partial \xi}\cdot\frac{\partial Y}{\partial \eta}$$

$$M_y = \frac{\partial Z}{\partial \xi}\cdot\frac{\partial X}{\partial \eta} - \frac{\partial X}{\partial \xi}\cdot\frac{\partial Z}{\partial \eta}$$

$$M_z = \frac{\partial X}{\partial \xi}\cdot\frac{\partial Y}{\partial \eta} - \frac{\partial Y}{\partial \xi}\cdot\frac{\partial X}{\partial \eta}$$

t = the thickness of membrane elements.

D = the elastic matrix of membrane elements.

2.1.3. The calculation of stiffness matrix of bar elements.

Using the same method, the stiffness of bar elements may be calculated as following,

$$K_B = AE_s \int_{\eta_1}^{\eta_2} [B]^T [L_B][B]\, r\, d\eta \qquad (3)$$

where, the local coordinate of membrane elements,

A = the areas of bar elements,

E = the elastic modulus of bar elements,

B = the geometric matrix of solid elements,

$[L_B]$ = the matrix of coordinate translation,

$$[L_B] = [l^2 \quad m^2 \quad n^2 \quad lm \quad mn \quad nl]$$

$$l = \frac{1}{r}\left(a\frac{\partial X}{\partial \xi} + \frac{\partial X}{\partial \eta}\right), \qquad m = \frac{1}{r}\left(a\frac{\partial Y}{\partial \xi} + \frac{\partial Y}{\partial \eta}\right), \qquad n = \frac{1}{r}\left(a\frac{\partial Z}{\partial \xi} + \frac{\partial Z}{\partial \eta}\right),$$

$$r = \sqrt{\left(a\frac{\partial X}{\partial \xi} + \frac{\partial X}{\partial \eta}\right)^2 + \left(a\frac{\partial Y}{\partial \xi} + \frac{\partial Y}{\partial \eta}\right)^2 + \left(a\frac{\partial Z}{\partial \xi} + \frac{\partial Z}{\partial \eta}\right)^2}$$

The idealized model using for 3D linear analysis consists of 448 nodes, 45 solid elements, 90 membrane elements and 20 bar elements. The results are shown in Fig. 2. 3. 4.

2.2 Elastic-plastic stress analysis by the finite element method [5]

In the nonlinear analysis, in order to research into the forming and developing of concrete's cracking, the axi-symmtric triangular elements and three dimensional constitutive relations were used.

2.2.1. The idealization of concrete solid

It was considered that the reinforced concrete solid may be approximately deal with as an orthotropy, and Poisson's ratio μ may be approached equal each other. In this case, for the problems of axi-symmetric, the elastic matrix may be taken as,

$$[D] = \frac{1}{(1-3\mu)(1+\mu)} \begin{bmatrix} (1-\mu)E_r & \mu\sqrt{E_r E_\theta} & \mu\sqrt{E_r E_z} & 0 \\ & (1-\mu)E_\theta & \mu\sqrt{E_\theta E_z} & 0 \\ & & (1-\mu)E_z & 0 \\ & \text{SYM} & & \frac{1}{4}[(1-\mu)E_r + (1-\mu)E_\theta - 2\mu\sqrt{E_r E_\theta}] \end{bmatrix} \qquad (4)$$

and there are four independent constants, E_r, E_θ, E_z, μ.

The basic assumptron in the orthotropic models is the coincidence of the axes of orthotropy and the principal stress directions. For concrete under tension or tension-compression state of stress, it is usually assumed that the behavior is linear elastic up to failure, and a linear-elastic fracture model may be used. For the compressive area, the equivalent uniaxial stress-strain relations are used. In this case, the tangential elastic modululi E_1, E_2 and E_3 are evaluated from an assumed stress-equivalent uniaxial strain relationship. In terms of the equivalent uniaxial strains, the generalized relations are written as [6]

$$\sigma_i = \frac{E_0 \varepsilon_{iu}}{1 + \left(R + \frac{E_0}{E_s} - 2\right)\frac{\varepsilon_{iu}}{\varepsilon_{ic}} - (2R-1)\left(\frac{\varepsilon_{iu}}{\varepsilon_{ic}}\right)^2 + R\left(\frac{\varepsilon_{iu}}{\varepsilon_{ic}}\right)^3} \qquad (5)$$

where

$$R = \frac{E_0\left(\frac{\sigma_{ic}}{\sigma_{if}} - 1\right)}{E_s\left(\frac{\varepsilon_{if}}{\varepsilon_{ic}} - 1\right)^2} - \frac{\varepsilon_{ic}}{\varepsilon_{if}}$$

More specifically, E_0 = the initial modulus of elasticity; σ_{ic} = the maximum(peak) stress, associated with direction i that occurs for the current principal stress ratio; ε_{ic} = the corresponding equivalent uniaxial strain; and σ_{if}, ε_{if} = the coordinates of some points on the descending branch of the stress-equivalent strain curve.

Differentiating Eq (5), with respect to ε_{iu}, the result is given by

$$E_i = E_0 \frac{1 + (2R-1)\left(\frac{\varepsilon_{iu}}{\varepsilon_{ic}}\right)^2 - 2R\left(\frac{\varepsilon_{iu}}{\varepsilon_{ic}}\right)^3}{\left[1 + \left(R + \frac{E_0}{E_s} - 2\right)\left(\frac{\varepsilon_{iu}}{\varepsilon_{ic}}\right) - (2R-1)\left(\frac{\varepsilon_{iu}}{\varepsilon_{ic}}\right)^2 + R\left(\frac{\varepsilon_{iu}}{\varepsilon_{ic}}\right)^3\right]^2} \qquad (6)$$

which defines the required moduli.

The five-parameter surface is used to obtain the strength values σ_{ic} in the present model [7].

The variations of the average shear stresses, τ_{mt} and τ_{mc}, along the tensile ($\theta = 0°$) and compressive ($\theta = 60°$) meridians respectively, are approximated by second-order parabolic expressions in terms of the average normal stress, σ_m, as follows, [8]

$$\frac{\tau_{mt}}{f'_c} = \frac{\rho_t}{\sqrt{5} f'_c} = a_0 + a_1\left(\frac{\sigma_m}{f'_c}\right) + a_2\left(\frac{\sigma_m}{f'_c}\right)^2 \qquad \text{at} \quad \theta = 0°$$

$$\frac{\tau_{mc}}{f'_c} = \frac{\rho_c}{\sqrt{5} f'_c} = b_0 + b_1\left(\frac{\sigma_m}{f'_c}\right) + b_2\left(\frac{\sigma_m}{f'_c}\right)^2 \qquad \theta = 60° \qquad (7)$$

in which τ_{mt} and τ_{mc} represent the value of the average shear stress τ_m for $\theta = 0°$ and $60°$, repectively; σ_m is the average normal stress; and ρ_t, ρ_c is the position vectors on the deviatoric plane. From which can be further defined the deviatoric stresses S_i and corresponding limited stresses σ_{ic}, a corresponding surface in the equivalent uniaxial strain space is used to define the three values of ε_{ic} that correspond to the σ_{ic}'s.

The idealized model using for nonlinear analysis consists of 476 nodes, 570 solid elements and 142 bar elements. The results are shown in Fig. 6, 7, 8.

2.2.2. The cracking element and calculating of unbalanced model force

The most important nonlinearity is tensile crack formation and propagation, coupled with associated stress redistributions. In the place nonlinear problems, as we described before [5], the stress state of every element under loading procedures may be divided into seven cases, they are: tension-tension; tension-compression; compression-compression; cracking-cracking; cracking-tension; cracking-compression and crushing etc. In the axi-symmetric nonlinear problems, the circumferential stress may be in tensile, cracking, compressive or crushing case. Considering all various possible combinations, the stress state of every element, in general, may be divided into twenty-eight possible cases.

The "modified Newton-Raphson method" is used to solve the nonlinear equations as the basic method. The iterative solution techniques for nonlinear analysis is shown in Fig. 9. The unbalanced force may be computed in the following ways,

1- Compute the set of element forces $\{S\}$ which equilibrate the internal stresses $\{\sigma\}$ in each element from the equation

$$\{S\} = \int [B]^T \{\sigma\} dV \qquad (8)$$

2- Assemble these element forces to find the external force which equilibrates the structure in this configuration.

3- The unbalanced force in them

$$(\Delta F_{MN})_{IJ} = \sum_e \int [B]^T \{\sigma\}_I dV - \sum_e \int [B]^T \{\sigma\}_{IJ} dV \qquad (9)$$

where I = A, B, C,...... denotes every loading step;
J = 1, 2, 3,...... denotes every iterative step in a certain loading step.

Thus, the first term of the right hand of Equ. (9) is represented the corresponding external nodal force which equilibrates the structure in each loading step, and the second one is represented the corresponding same one in each iterative step of a certain loading step.

The convergence criteria of iteration, the iterative method and the accelerative method are as the same as described in the another paper. [5]

2.3. The ultimate load calculation

In the ultimate load calculation, the ultimate load of the vessel was calculated by using the yeild line method. The mechanism of the failure model and the rupture lines under ultimate loading were determined by the test, as shown in Fig. 10. Balancing the stress on the enterior loading, the analysis of the ultimate load of the vessel was performed. The final ultimate load using this method was 249.5kg/cm^2.

3. Test and its results [1]

3.1. The arrangement of instrumentation

The model of PCRV were instrumented for measurements of concrete strains, steel strains, surface deformations of model and for detection of cracking of concrete.

Twenty-eight mechanical dials and the same number of electronic transducers were arranged around the model to measure surface deformations.

One hundred and ten resistance wire strain gauges were bonded to the free concrete surface to measure surface strains. About one hundred resistance wire strain gauges were used to measure strain of the liner. About four hundred polyester mold gauges, which were collected in groups with 2 to 4 in each, forming a rosetts for determination of principal directions, were embedded into the concrete to measure internal strains of concrete. The measuring length of these gauges were 40mm.

Eight loading transducers were placed under the anchorages to measure the forces in the prestressing tendons.

Brittle, electric conducting painting were used as crackindicators to indicate the cracking of concrete on the upper surface and the waist of barrel. Some special crackindicators, which were made of pencil wick, were embedded into the internal corner.

The measurements were performed automatically by a 256 channel strain-gauge scanner, collecting the signals from strain-gauges crackindicators, pressure transducers and differential transformers. The measurement of mechanical dials was performed manually.

During the time of ultimate pressure test, four cameras arranging in different positions were used to recorded the whole experimental precess and especially to catch the moment of jetting water.

3.2. Elastic test

Several times loading experiment were performed under 55kg/cm^2 (1.25 times design pressure). It was shown that the linear relations were obtained between the surface deformations, strains and interior pressure, and the good repeatability was maintained, as shown in Fig. 4.

3.3. Cracking test

The first crack on the surface was observed at 79-83kg/cm^2, as shown in Fig. 11 . This crack extended as the loading was increasing. When the loading was increased at 100kg/cm^2, the first crack was 0.09mm in width and 40cm in length. When it was unloaded, the first crack could be closed. This crack would be observed again, when the vessel was loaded repeatedly, but at the lower loading. As the loading was increased, the cracks were observed at the central part of the top slab and at the waist of barrel, as shown in Fig. 11 . When the loading was increased at 100kg/cm^2 and it was maintained in 3.5 hours, many new cracks were observed continually. When it was at 130kg/cm^2, the first crack was 80cm in length and 0.2mm in width. In addition, many new cracks would be obtained.

3.4. Ultmate pressure test

Considering the higher safety of model, the prestressed tendons were decreased by 10%.

At a pressure of about 160kg/cm^2, at the mid-high of the wall, there were many cross cracking, as shown in Photo 1 . The cracks of the top slab were extended. The sound of slipping of prestressed tendon in its conduit and the sound of relaxing of anchor could be heard.

The final ultimate load was occured at 191kg/cm^2 when the interior pressure water was suddenly jetted out through the barrel, photo 2 . The end slab was seriously cracked and deformed, but not failed. The deflection at the centre of the end slab was more than 4mm.

4. Conclusion

1- The model was elastic up to a pressure of about 1.25 times design pressure (55kg/cm^2), during this loading period the good repeatability was maintained. The measured deflections and strains at 51kg/cm^2 (1.15 times design pressure) were good agree with those obtained in the tests.

2- The surface cracking load was 79kg/cm^2.

The cracking safe factor was 1.8 which was larger than the prediction value 1.25. After 100kg/cm^2 elastics-plastic behaviour was appeared in all parts of the vessel.

3- The failure was occured at the upper part of barrel. The final failure load was about 219kg/cm^2 which was 5.2 times design pressure. It was apparent that the high safety of PCRV was ensured.The final failure was abrupt in form of jetting out pressurised water, but warning was given by surface cracks and progressive deformations.

4- There was generally good agreement in both displacement and strain between the test results and 3D linear calculating and axi-symmetric (3D) nonlinear analysis. It was clear that, the validity of the analytical methods which the authors developed was confirmed, and on the other hand the predication of PCRV was also verified.

References

/ 1 / D.Mcd.Eadie, D. J. Bell, Testing the One-tenth Seale Model of the Hinklay Point B and Hunterston B Power Station PCRV, Model Techniques for PCRV Proceeding of the Conf. B. W. E. S. in London, July (1969)

/ 2 / Wang Chung-zhi, Li Jing-cai, Wang Tai-jun, Gu shu-hua, The Design and Experimental Study on 1/10th Scale Model of PCRV(in Chinese).The 1st SMiRT in China, 1978

/ 3 / O. C. Zienkiewicz, et al., Finite Element Method in the Analysis of Reactor Vessels, Nuclear Engineering and Design, Vol. 20, No. 2, July 1972.

/ 4 / He Shu-yan, He kang-hui, Xiong Dun-shi, Wang Tai-jun, The Three-Dimensional Isoparametric Finite Element Program Method of PCRV(in Chinese)Nuclear Power Engineering, No. 2, 1982

/ 5 / Wang Tai-jun, Xiong Dun-shi, Liu Jun-jie,Nonlinear Finite Element Analysis of Plane Structures in Reinforced Concrete, 8th SMiRT, 1985.

/ 6 / Alwa A. Elwi and David W. Murray, A 3D Hypoelastic Concrete Constitutive Relationship, Proceedings of the A.S.C.E. Journal of Engineering Mechanics Division. Vol. 105,No.EM4, Aug. 1979.

/ 7 / Willam K. J., and Warnke,E.P., Constitution Models for the Triaxial Behavior of Concrete, International Association of Bridge and Structural Engineers Seminer on 'Concrete Structures Subjected to Triaxial Stresses', Paper 3-1, Bergamo, Italy, May 17-19,1974.

/ 8 / Chen,W.F., and Saleeb,A.F., Constitutive E uations for Engineering Materials Vol.1, 'Elasticity and Modelling', 1981, New York.

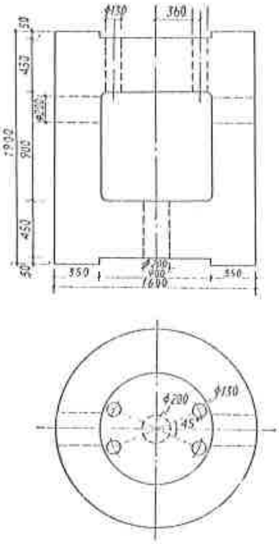

Fig. 1, Size of model.

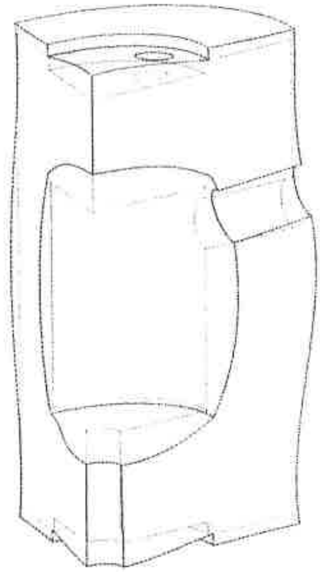

Fig. 2, Deformation at 51 kg/cm^2.

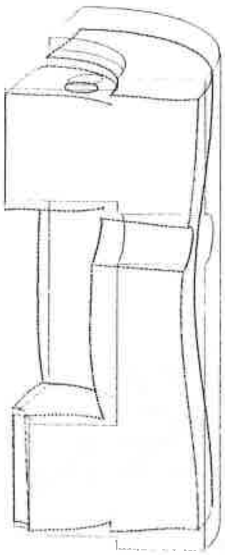

Fig. 3, Deformation at prestressed load.

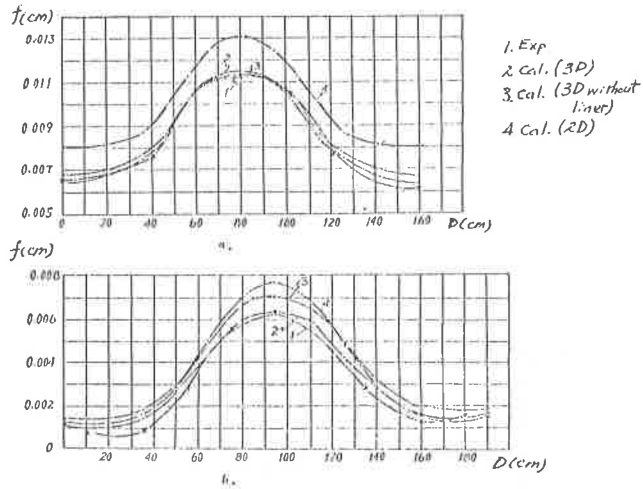

Fig. 4, Deflections in the 51 kg/cm^2 test.
a- Flexural curve of the top slab,
b- Flexural curve of barrel.

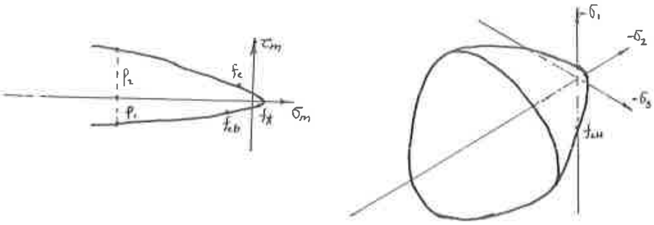

Fig. 5, The ultimate strength surface.
a- General view,
b- The rendulic view.

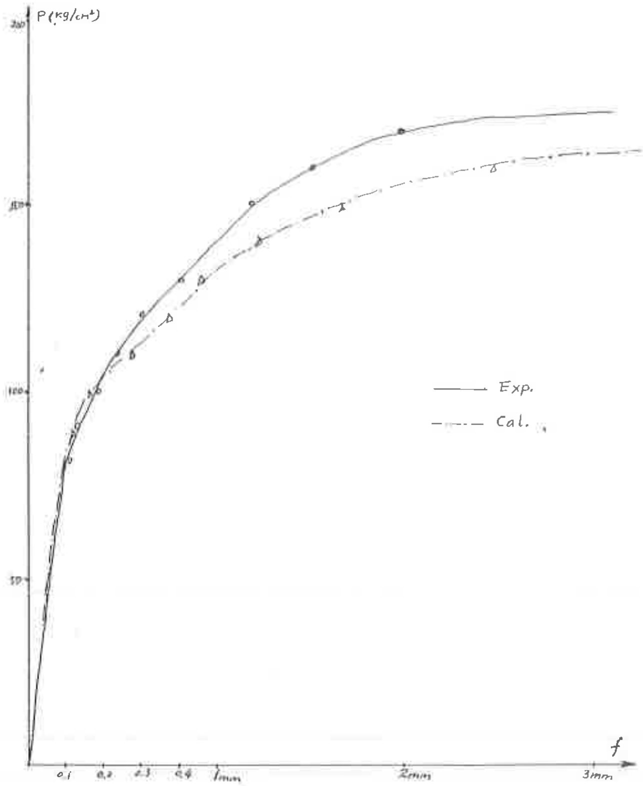

Fig. 6, Deflections in the ultimate pressure test.

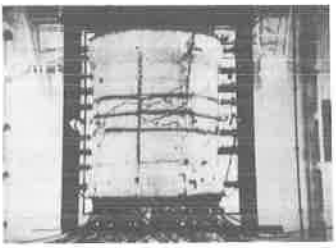

Photo 1, Surface cracks of vessel.

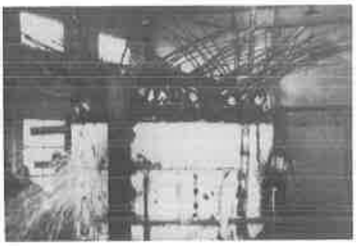

Photo 2, The moment of jetting water.

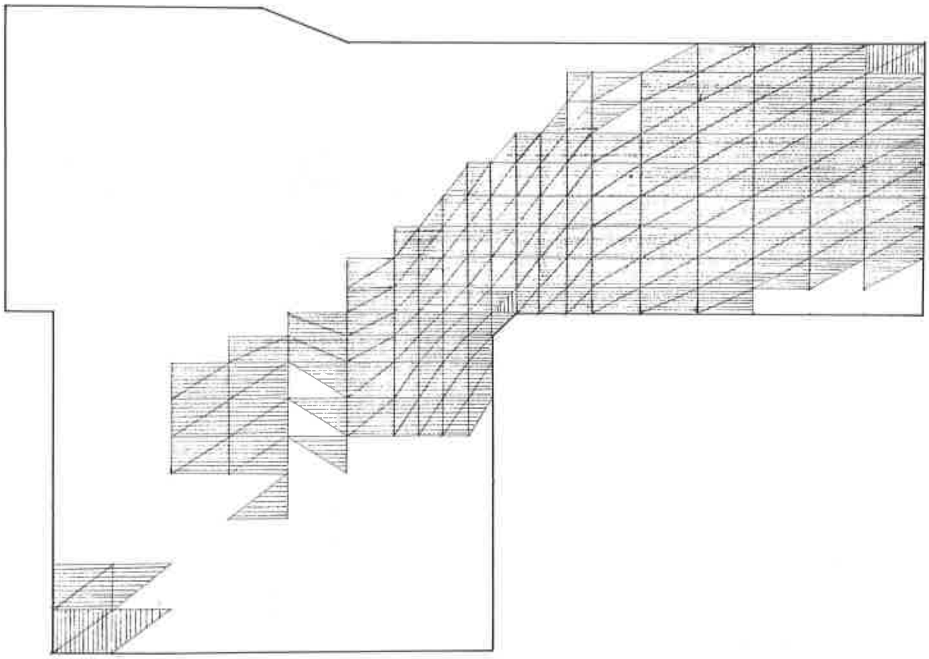

Fig. 8, Cracking zone at 180 kg/cm^2.

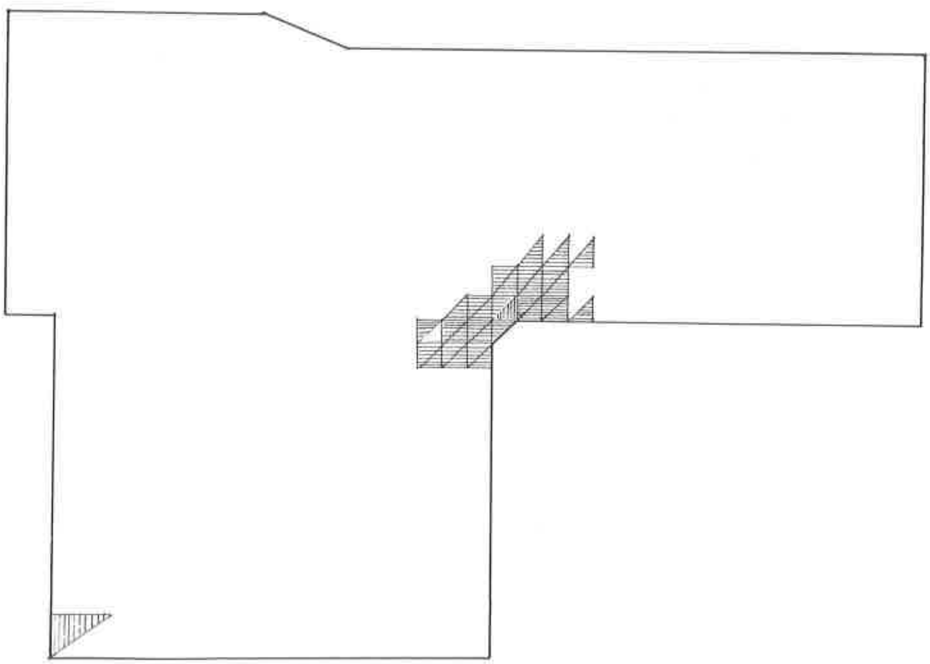

Fig. 7, Cracking zone at 100 kg/cm^2.

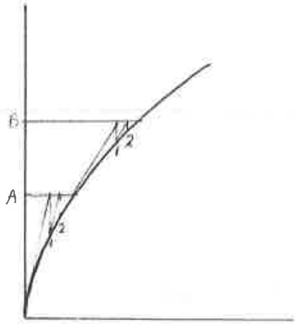

Fig. 9, Iterative solution technique.

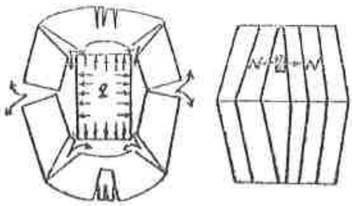

Fig. 10, Model for ultimate load analysis.

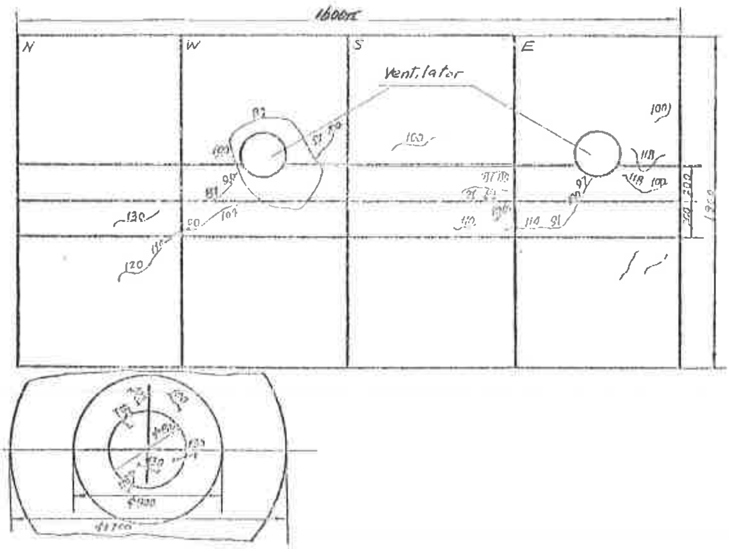

Fig. 11, Extension of cracks on the slab and barrel.